Line excited curved panels radiation at high frequency by a power flow method

V. Cotoni, A. Le Bot, M.N Ichchou and L. Jezequel
Laboratoire de Tribologie et Dynamique des Systèmes - UMR CNRS 5513
École Centrale de Lyon - 36, av Guy de Collongue - 69131 Écully, France
e-mail: cotoni@mecasola.ec-lyon.fr

Abstract

A power flow integral approach is used to derive the vibroacoustic behaviour of semi-infinite curved panels excited by line forces. Energy quantities inside the subsystems and coupling between subsystems are locally described. Energy fields are derived using a propagative decomposition. Due to the curvature, every waves have normal and tangential components, and may radiate power. Radiation is located along supersonic waves travel and on structural discontinuities such as edges or excitation lines.

1 Introduction

Power flow methods have motivated several researches in the last few decades [1, 2, 3]. Dealing with the same energy variables as SEA, these methods are dedicated to the high frequency range where classical kinematic approaches are limited due to the increasing computation time. Another advantage of these methods is to give averaged results of the very sensitive responses of systems in high frequencies. Unlike SEA, power flow methods are interested in describing energy densities inside the systems and local power balances are used on boundaries and inside the systems. Assuming that propagative fields are uncorrelated, an integral formulation was developped and successfully applied to problems involving coupling between systems of same dimension [3].
This paper deals with vibroacoustic coupling applied to cylindrical shells. Classical approaches are used to perform angular harmonics decompositions to derive the coupled system. In the spirit of energy methods, a propagative decomposition based on the so-called helical waves [4, 5] is used here to express the local power exchanges. In high frequency, two waves principally interfere in the energy balances. Because the curvature radius becomes large compared to the wavelenghts, they correspond to the flexural and longitudinal waves of the equivalent flat structure. Two kinds of radiation processes are involved in the power flow exchanges: power may be radiated by supersonic waves and diffracted on structural discontinuities such as edges or excitation points.

The second section begins with the calculation of propagative parameters. Then, canonical problems involving the different radiation processes are derived and the corresponding local power balances are expressed. The results are introduced in the integral energy formulation in the third section. The last section shows some numerical comparisons between energy and reference kinematic calculations.

2 Canonical problems

Given a semi-infinite cylindrically baffled curved panel excited by axially line forces (Figure 1), due

to the semi-infinite geometrie, the problem reduces to a bidimensional analysis. The structure material is charaterized by the Young's modulus E, the Poisson coefficient ν, the thickness h and the density ρ_s. We note R the radius of the cylinder, s the curvilinear abscissa, r the radial coordinate, u and v the tangential and normal displacements, and p the acoustical pressure. Excitations are line transverse forces F_0, moments M_0 and tangential forces N_0. The fluid is characterized by the density ρ_a and the sound velocity c_a. There is no fluid on the internal side of the panel. The time harmonic term $e^{j\,\omega t}$ is omitted in the following developpements.

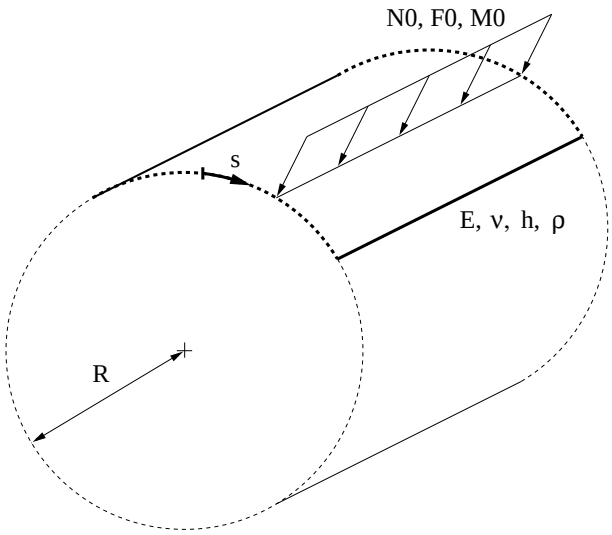

Figure 1: Studied geometry

μ denotes the ratio $h^2/12$ and D is the stiffness written $Eh^3/12(1-\nu^2)$. k_f is the flexural real-valued wavenumber of the equivalent flat plate: $k_f^4 = \rho_s h\omega^2/D$. k_l is the longitudinal wavenumber of the equivalent flat plate: $k_l^2 = (1-\nu^2)\rho_s\omega^2/E$. k_a is the acoustical wavenumber: $k_a = \omega/c_a$. Starting with the Timoshenko's model [6] for shells (more complete than Donnell's one), equations describing the line excited fluid loaded cylindrical shell are derived as follow

$$\begin{cases} \dfrac{d^4v}{ds^4} - k_f^4 v + \dfrac{v}{\mu^2 R^2} - \dfrac{1}{R}\dfrac{d^3u}{ds^3} + \dfrac{1}{\mu^2 R}\dfrac{du}{ds} = \dfrac{F_0}{D}\delta(0) + \dfrac{M_0}{D}\dfrac{d\delta(0)}{ds} - \dfrac{p_{r=R}}{D} \\ \dfrac{d^2u}{ds^2} + k_l^2 u + \dfrac{\mu^2}{R^2}\dfrac{d^2u}{ds^2} - \dfrac{\mu^2}{R}\dfrac{d^3v}{ds^3} + \dfrac{1}{R}\dfrac{dv}{ds} = \dfrac{N_0}{Eh/(1-\nu^2)}\delta(0) \\ (\nabla^2 + k_a^2)p = 0 \\ \dfrac{\partial p}{\partial r}_{r=R} = \rho_a\omega^2 v \end{cases} \tag{1}$$

Equations must be completed by the Sommerfeld radiation condition at infinity for the pressure p and by the boundary conditions for the displacements u and v. The structural time-averaged energy is the sum of longitudinal and flexural energies (noted W_l and W_f)

$$W_l = \frac{1}{4}\rho_s h\omega^2|u|^2 + \frac{1}{4}\frac{Eh}{1-\nu^2}\left|\frac{v}{R} + \frac{du}{ds}\right|^2 \qquad W_f = \frac{1}{4}\rho_s h\omega^2|v|^2 + \frac{1}{4}D\left|\frac{d^2v}{ds^2} - \frac{1}{R}\frac{du}{ds}\right|^2 \tag{2}$$

The time-averaged power flow is expressed in term of tangential and transverse forces N and T, and moment M, as follow

$$I = \frac{1}{2}\Re\left(j\omega\left[Tv^* + M\frac{dv^*}{ds} + Nu^* - M\frac{u^*}{R}\right]\right) \tag{3}$$

where * denotes the complex conjugate and $\Re$ the real part.

Starting with the energy definitions (2-3), we now derive the system (1) in order to determine the power exchanges between the structure and the acoustical medium in some particular canonical radiation problems. The first step is to find the propagative parameters, by solving the dispersion equation.

2.1 Dispersion equation

Displacements and pressure are expressed in propagative forms, $u(s) = ae^{-j\,ks}$, $v(s) = be^{-j\,ks}$ and $p(r,s) = c(r)e^{-j\,ks}$, where k denotes the fluid-loaded curved structure wavenumber. The Helmholtz equation of (1) written in cylindrical coordinates leads to the Hankel equation for $c(r)$. The pressure is thus written

$$p(r,s) = d\,H_{kR}(k_a r)\,e^{-j\,ks} \tag{4}$$

where H_{kR} denotes the Hankel function of order kR and of the second kind, in respect with Sommerfeld radiation conditions. The coupling condition gives the value of d. Substituting the propagative forms in system (1) with homogeneous conditions leads to a matricial equation involving $\mathcal{A}$

$$\mathcal{A} = \begin{bmatrix} \frac{-j}{R}(k^3 + \frac{k}{\mu^2}) & k^4 - k_f^4 + \frac{1}{\mu^2 R^2} + \frac{\rho_a k_f^4}{\rho_s h k_a}\frac{H_{kR}(k_a R)}{H'_{kR}(k_a R)} \\ k^2 - k_l^2 + \frac{\mu^2}{R^2}k^2 & \frac{-j}{R}(\mu^2 k^3 + k) \end{bmatrix} \tag{5}$$

The corresponding dispersion equation is $\det(\mathcal{A}) = 0$. We note k_i the solutions of this dispersion equation. Amplitudes of displacements and pressure for the wave i are related by:

$$\frac{b_i}{a_i} = \varepsilon_i = \frac{k_l^2 - k_i^2(1+\frac{\mu^2}{R^2})}{\frac{j}{R}(\mu^2 k_i^3 + k_i)} \qquad and \qquad \frac{d_i}{b_i} = \nu_i = \frac{\rho_a \omega^2}{k_a H'_{k_i R}(k_a R)} \tag{6}$$

where H' denotes the derivative of the Hankel function with respect to argument. The present coupling with air is considered light and we are interested in the solutions deriving from the propagative solutions of the in vacuo structure. If the radius tends to infinity, these in vacuo solutions are the longitudinal and flexural wavenumbers of the flat plate (k_l and k_f previously defined). Approximate solutions of the dispersion equation may be derived in the case of light fluid loading by using the Debye expansions of Hankel functions.

Using the calculated wavenumbers k_i, we now derive several radiation mechanisms for each wave: the purpose of the following canonical calculations is to characterize the local power balances for each radiation process.

2.2 Direct radiation

Radiation emanating from the line force is first considered. Tangential and normal point admittances of the infinite fluid loaded panel are noted $U(\gamma)$ and $V(\gamma)$. Tangential and normal velocities and

pressure are thus discribed by the Fourier integrals:

$$\dot{u}(s) = \int_{-\infty}^{+\infty} U(\gamma)\, e^{j\,\gamma s} d\gamma \qquad\qquad \dot{v}(s) = \int_{-\infty}^{+\infty} V(\gamma)\, e^{j\,\gamma s} d\gamma \tag{7}$$

$$p(r,s) = \int_{-\infty}^{+\infty} \frac{j\rho_a\omega}{k_a} \frac{H_{\gamma R}(k_a r)}{H'_{\gamma R}(k_a R)}\, V(\gamma)\, e^{j\,\gamma s} d\gamma \tag{8}$$

Classical residue calculations of integrals (7) give the contributions to the displacement of the different propagative waves. The power being injected in each wave may thus be determined by expressing the transverse, normal and rotation velocities due to each wave k_i at origin.

$$P_i = \frac{1}{2}\Re\left(\dot{u}_{k_i}(0) N_0^* + \dot{v}_{k_i}(0) F_0^* + \frac{d\dot{v}_{k_i}}{ds}(0) M_0^*\right) \tag{9}$$

The pressure being radiated is the branch cut contribution to the pressure integral (8). Its calculation is performed using the stationnary phase method with the large argument expansions of Hankel functions. The stationnary point is $\gamma_0 = k_a \sin\theta$, θ being the cylindrical angle ($d\theta = Rds$) and the pressure being radiated expressed in cylindrical coordinates is written as follow

$$p(r,\theta) = j\rho_a\omega \left(\frac{2\pi}{k_a r}\right)^{1/2} V(k_a \sin\theta)\, e^{j\,k_a(r + R\cos\theta + \pi/4)} \tag{10}$$

The specific intensity, that is the power being radiated into an elementary solid angle about θ, is

$$P_{rad}(\theta) = 2\pi\rho_a\omega\, |V(k_a \sin\theta)|^2 \tag{11}$$

The total power being supplied in the coupled system is the sum of each structural wave injected power and the radiated power: $P_{inj} = \sum_i P_i + \int_{-\pi/2}^{\pi/2} P_{rad}(\theta) d\theta$. $\Sigma^{exci}(\theta)$ and Σ_i^{struc} denote the ratios of the specific intensity in θ direction and the structural power supplied to each wave i, over the total power being injected

$$P_{rad}(\theta) = \Sigma^{exci}(\theta)\, P_{inj} \qquad and \qquad P_i = \Sigma_i^{struc}\, P_{inj} \tag{12}$$

2.3 Edge radiation

A structural wave impinging on a discontinuity is diffracted in the acoustical medium. The problem of power radiated when a wave is reflected on a boundary condition is calculated similarly as previous problem: under the light fluid hypothesis, the Fourier transform of the structural in vacuo displacement field is known and used to calculate the pressure being diffracted, by a stationnary phase calculation.

If V_i denotes the Fourier transform of the normal velocity field due to an impinging wave i, the pressure is written

$$p_i(r,\theta) = j\rho_a\omega \left(\frac{2\pi}{k_a r}\right)^{1/2} V_i(k_a \sin\theta)\, e^{j\,k_a(r + R\cos\theta + \pi/4)} \tag{13}$$

The reflected displacement field is composed of every wave types: $v^r(s) = \sum_j r_{ij} e^{j\,k_j s}$. Deriving the boundary conditions gives the reflexion coefficients r_{ij} involved in V_i expression. Starting with expression (3), the power flux $\mathcal{P}_i^{\pm}$ carried by the wave i travelling in $\pm$ direction are expressed. The

in vacuo energy reflection coefficients are then written as ratios of the incident power from wave i over the reflected power in wave j: $R_{ij}^{vacuo} = \dfrac{\mathcal{P}_j^-}{\mathcal{P}_i^+}|r_{ij}|^2$.

With the coefficients r_{ij} and the equation (13) the diffracted pressure due to an impinging wave i is determined. The specific intensity is derived in terms of incident flux, $I_i^+(0)$, and by taking into account the directivity

$$P_i^{rad}(\theta) = \Sigma_i^{edge}(\theta)\, I_i^+(0) \qquad with \qquad \Sigma_i^{edge}(\theta) = 2\pi\rho_a\omega\, \frac{|V_i(k_a \sin\theta)|^2}{\mathcal{P}_i^+} \tag{14}$$

In order to respect the power balance at the edge, in vacuo energy reflection coefficients must be modified by taking into account the radiated power. We assume that all fluid loaded reflection coefficients are similarly reduced

$$R_{ij} = (1 - \Pi_i^{rad}) R_{ij}^{vacuo} \qquad with \qquad \Pi_i^{rad} = \int_{-\pi/2}^{\pi/2} \Sigma_i^{edge}(\theta) d\theta \tag{15}$$

2.4 Supersonic wave radiation

The power flux radiated by a propagative wave is $\vec{I}_a = 1/2\Re(p[\vec{\nabla}p/\rho_a\omega]^*)$. Starting with the pressure expression (4), directivity and magnitude of the power being radiated are determined. For a propagative wave, the directivity is defined by the angle with the normal to the surface $\varphi_i^{rad} = \arctan\Re[-jk_iH_{k_iR}(k_aR)/k_aH'_{k_iR}(k_aR)]$ and the magnitude is the projection of $\vec{I}_a$ on the normal to the structure. It is shown to be proportional to the structural power flow. The specific intensity may thus be written in terms of structural flux and by taking into account the directivity, as follow

$$P_i^{rad}(s,\varphi) = \Sigma_i^{surf}\, \delta(\varphi - \varphi_i^{rad})\, I_i(s) \qquad with \qquad \Sigma_i^{surf} = \frac{\rho_a\omega^3}{2}\Re\left(\frac{-jH_{k_iR}(k_aR)}{k_aH'_{k_iR}(k_aR)}\right)\frac{|\varepsilon_i|^2}{\mathcal{P}_i} \tag{16}$$

This proportionality relation shows that the fluid coupling induces damping to the structure when the real part of expression (16) is non zero: using high frequency expansions of Hankel functions, this is shown to occur when structural waves are supersonic ($k_i < k_a$). The radiated flux directivity depends on the propagation direction: the flux I_i^+ (resp. I_i^-) radiates with the angle $+\varphi_i^{rad}$ (resp. $-\varphi_i^{rad}$).

3 Energy derivation of coupled system

The energy formulation has been already applied to multipropagative systems [7, 8]. Propagative waves are assumed uncorrelated inside the domain. Their energetic contributions are solved independantly and simply summed. The coupling between them only appears at the edges where an incident wave may generate several reflected wave types (coefficients $R_{i,j\neq i}$ are non zero).

As calculations are performed with ligth fluid, we only keep the waves coming from the in vacuo curved structure: two waves corresponding to flexural and longitudinal waves of the equivalent flat structure have a propagative form for the kind of structure radius and frequency range which are considered in the applications.

3.1 Integral energy formulation

The main hypothesis of the integral energy formulation is to consider that propagative fields are uncorrelated, which makes the energy quantities additive. Then, for each propagative wave, energy fields are the sum of direct contributions emanating from sources located inside the system and secondary contributions from sources located on the boundaries. Energy kernels used to describe each source contribution are solutions of the local power balance for a point excited infinite domain. For isotropic, linear and lightly damped systems, kernels corresponding to energy density G and power flow density $\vec{H}$ are expressed in radial coordinates [3]

$$G(r) = \frac{1}{\gamma_0 c}\frac{e^{-mr}}{r^{n-1}} \qquad \vec{H}(r) = \frac{1}{\gamma_0}\frac{e^{-mr}}{r^{n-1}}\,\vec{u}_r \tag{17}$$

with n being the dimension of the system, γ_0 the solid angle of the space, c the group velocity of the waves and m the attenuation factor related to the hysteretic damping coefficient by $m = \eta\omega/c$. These kernels concern propagative fields only: evanescent fields that do not carry any power are not included in the energy description. Energy and power flow densities inside the system are written in terms of direct (ρ) and boundary (σ) sources contributions as follow

$$W(M) = \int_\Omega \rho(S, \vec{u}_{SM})\, G(S, M)\, dS + \int_{\partial\Omega} \sigma(P, \vec{u}_{PM})\, G(P, M)\, dP \tag{18}$$

$$\vec{I}(M) = \int_\Omega \rho(S, \vec{u}_{SM})\, \vec{H}(S, M)\, dS + \int_{\partial\Omega} \sigma(P, \vec{u}_{PM})\, \vec{H}(P, M)\, dP \tag{19}$$

Direct sources are the injected powers and are supposed to be known. Magnitudes of the secondary sources are to be determined by applying the local power balance on the boundaries as will be illustrated for radiation problems in the next section.

3.2 Structure calculation

Due to the semi-infinite geometry (see Figure 1), the structure reduces to a one-dimensional system. It is described by two propagation waves. Fluid loading is taken into account by modifying the following parameters

- The injected power must include the direct radiation appearing on the excitation line (see equation (12)).
- Due to the edge radiation, energy reflection coefficients are modified. For every incident wave i, the sum of the reflected flux is not equal to the incident flux anymore, and edges act as dissipative boundaries: $\Sigma_j R_{ij} < 1$ (see equation (15)).
- For supersonic propagation waves, continuous radiation induces damping introduced in the attenuation factor m_i by adding the quantity Σ_i^{surf} from equation (16).

The structural energy is described by four boundary sources corresponding to both waves, on both extremities. The power balance on the edge is written $P_i^{refl} = R_{ii}P_i^{inc} + R_{ji}P_j^{inc}$ where P_i^{refl} denotes the power reflected by the boundary with the wave i and due to the incident powers P_i^{inc} and P_j^{inc} carried by the waves i and j. Expressed in terms of direct and boundary sources by following expression (19), a linear system on the four edge sources is obtained. Then, flexural and in-plane energies may be derived using equations (2) and (18) and by summing each wave contributions.

3.3 Acoustical medium calculation

Acoustical energy fields are derived by introducing power sources located on the structure. There is no acoustical direct sources and expression (18) for the acoustical medium reduces to an integral over the structure

$$W_a(M) = \int_{\Omega_s} \sigma_a(P, \vec{u}_{PM}) \frac{e^{-m_a PM}}{c_a PM} \, dP \tag{20}$$

The direct radiation is first derived. Starting with expression (12), the boudary source corresponding to the power being radiated by the excitation discontinuity is

$$\sigma_a(S, \vec{u}_a) = \Sigma^{exci}(\theta_{P_0}) P_{inj} \tag{21}$$

θ_{P_0} is the cylindrical angle corresponding to $\vec{u}_a$ direction in the frame centered on the excitation point P_0 (see the Figure 2 for notations).

The radiation of the edges is derived similarly. Using edge efficiencies (14) the secondary sources on left and right extremities (noted P_l and P_r on Figure 2) are written in terms of impinging flux carried by each wave

$$\sigma_a(P_l, \theta_{P_l}) = \sum_i \Sigma_i^{edge}(\theta_{P_l}) I_i^-(P_l) \qquad and \qquad \sigma_a(P_r, \theta_{P_r}) = \sum_i \Sigma_i^{edge}(\theta_{P_r}) I_i^+(P_r) \tag{22}$$

θ_{P_l} (resp. θ_{P_r}) denotes the cylindrical angle in the frame centered on P_l (resp. P_r). I_i^- (resp. I_i^+) is the structural flux traveling from right to left (resp. left to right).

The radiation of supersonic waves is introduced in the integral power flow formulation by surface sources located along the whole structure. Boundary sources are expressed in terms of surface efficiencies of each wave (equation 16). Two boundary sources σ_a^- and σ_a^+ corresponding to the two propagation directions are considered

$$\sigma_a^{\pm}(P, \theta_P) = \sum_i \Sigma_i^{surf} I_i^{\pm}(P) \delta(\theta_P \mp \varphi_i^{rad}) \tag{23}$$

θ_P denotes the cylindrical angle in the frame centered on point P, describing the whole structure. Due to the Dirac function, the energy derivation is not as trivial as previous cases. Substituting (23) into integral (18), two discrete contributions corresponding to both propagation directions are obtained per supersonic wave. For P describing the structure and M the acoustic, we note θ the angle between OM and OP, and r the radial coordinate of M ($r = OM$). Considering that $dP = ds = Rd\theta$, the following relation holds

$$\frac{d\theta_P}{d\theta} = \frac{r}{PM^2}(r - R\cos\theta) \tag{24}$$

Changing the integration variable from dP to $d\theta_P$, the energy density due to the supersonic wave i becomes

$$W_{ai}(M) = \Sigma_i^{surf} \left[I_i^+(P_i^+) \frac{e^{-m_a P_i^+ M}}{c_a} \frac{R}{r} \frac{P_i^+ M}{(r - R\cos\theta)} + I_i^-(P_i^-) \frac{e^{-m_a P_i^- M}}{c_a} \frac{R}{r} \frac{P_i^- M}{(r - R\cos\theta)} \right] \tag{25}$$

where P_i^+ and P_i^- are the points of the structure radiating in M with the angle $+\varphi_i^{rad}$ and $-\varphi_i^{rad}$. They may exist or not. For one supersonic wave, the point M may thus be in a shadow zone or receive 1 or 2 rays.

Using the assumption of uncorrelated waves, the whole acoustical energy field is the sum of each sources contribution, corresponding to the different radiation processes (21, 22 and 23).

4 Numerical simulations

Power flow calculations are now compared to kinematic frequency averaged results. Applications are performed with an aluminium ($E = 0.72\,10^{11}\,N\,m^{-2}$, $\nu = 0.3$, $h = 2\,mm$, $\rho_s = 2800\,kg\,m^{-3}$) shell of radius $R = 0.95\,m$ with air ($\rho_a = 1.3\,kg\,m^{-3}$, $c_a = 340\,m\,s^{-1}$) on the external side. The panel is 1.5 meter large which corresponds to an arc of $\pi/2$ radians. Excitations are line transverse and tangential forces. The wave coming from the longitudinal flat wave is always supersonic. The one coming from the flexural wave is subsonic below the critical frequency ($f_c \sim 6\,kHz$) and supersonic above. Both frequency domains are investigated.

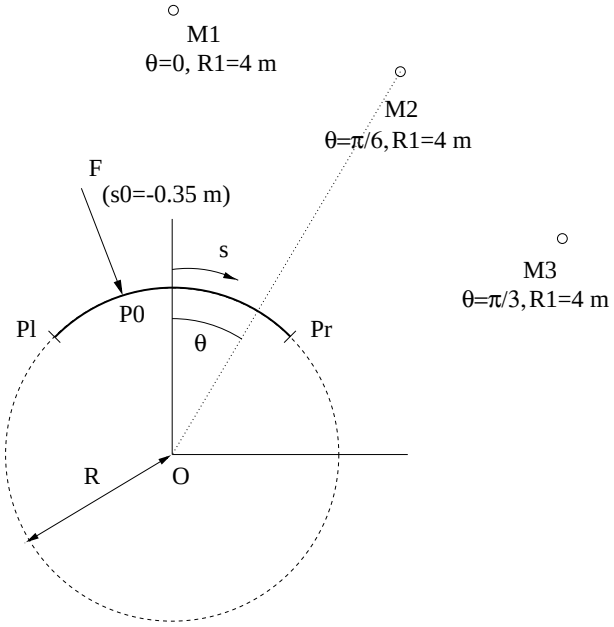

Figure 2: Calculated geometry

Calculations start at $800\,Hz$ and cover 5 octave bands (up to $25600\,Hz$). The structure is simply supported, and excited on $s_0 = -0.35\,m$. Energy variations are investigated for one structural point and three acoustical points, $M_{1,2,3}$ located on $\theta = 0,\ \pi/6,\ \pi/3$ on the circle of radius $4\,m$ (see Figure 2). At the starting frequency, there is only 0.22 longitudinal wavelenghts along the structure. The system is not in the high frequency hypothesis and strong modal effects may appear. As the power flow approach neglects the interferences between propagative fields, these effects are not considered by the energetic calculations and moderate results may be expected. As the frequency increases, both flexural and longitudinal waves have several wavelenghts along the panel and the system respects the high frequency hypothesis.

Results concerning the transverse force excitation are presented on Figures 3 and 4, and the case of the tangential force on Figures 5 and 6. The abscissa is the frequency divided by the critical frequency, and the ordinate is the energy density divided by the injected power. The frequency reference variations are ploted with grey lines. In both cases, the power flow calculations (thick lines) are in good agreement with the averaged kinematic results (–o–), for the acoustical, flexural and longitudinal energies. The good agreement for structural energies shows that the mode conversion occuring on the edges is well predicted by the local power flow analysis.

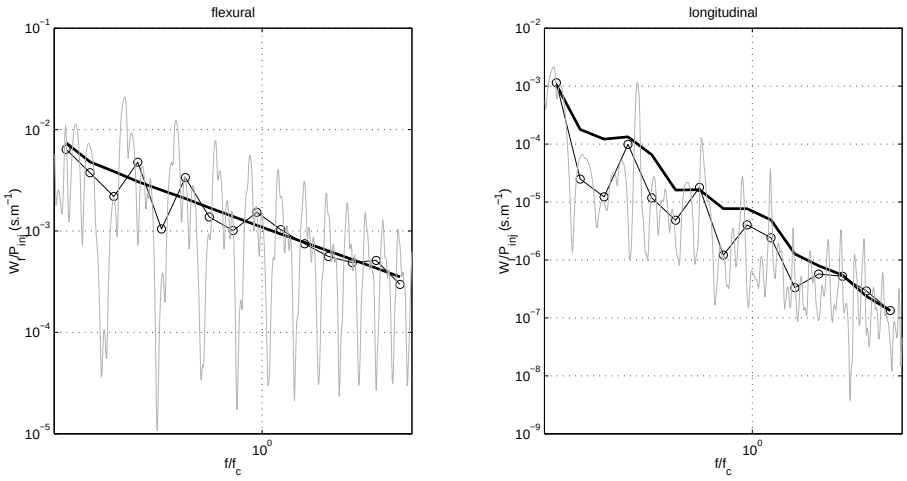

Figure 3: Frequency flexural and longitudinal energies variations for the transverse excitation case; grey lines are the kinematic calculations; –o– lines are the 1/3 octave band averaged kinematic calculations; thick lines are the power flow results

The changes of radiation process of the flexural waves becoming supersonic above the critical frequency is visible on Figures 4 and 6. In the case of the transverse excitation (Figure 4), the flexural wave is well excited and is the major contributor to radiation. Anyway, the supersonic longitudinal wave must be taken into account, especially below the critical frequency where the flexural wave radiation emanates from discontinuities only and is less efficient. In the case of the tangential excitation (Figure 6), the radiation of the longitudinal wave is still important below the critical frequency. This wave having a large wavelenght, the reference acoustical energy (grey line) has a modal behaviour in this low frequency range. This is not the case above the critical frequency where flexural radiation becomes predominant, flexural waves having a much shorter wavelenght. A detailed analysis may be performed on the diffraction sources located on the edges and excitation points. In particular, shadow effects due to the curvature are well described by the power flow calculations.

5 Conclusion

This study demonstrates the ability of the integral power flow method to give the spatial repartition of the acoustical energy field radiated by curved structures. The exterior acoustical medium, where the field is not diffuse is spatially described by using realistic directivities for the boundary power sources. The present analysis uses two propagative waves corresponding to the flat structure longitudinal and flexural waves. Due to the curvature, both waves have normal and tangential displacement components and may radiate power. Waves are assumed to propagate uncorrelated and coupling between them occurs on edges reflections (conversion mode phenomenon).

The longitudinal wave is well excited by tangential forces and most of its energy is due to tangential displacements. Despite its small normal contribution, it radiates efficiently because it is always supersonic. The flexural wave, well excited by transverse forces or moments may be subsonic or supersonic. Power is also radiated by diffraction of the elastic waves on the structural discontinuities such as edges or excitation point.

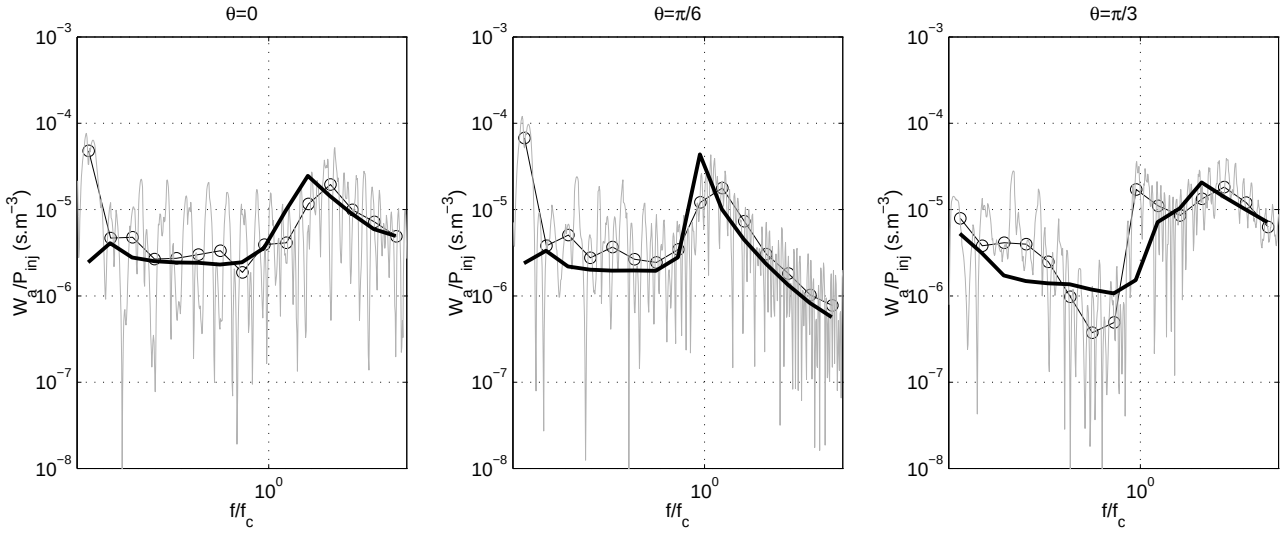

Figure 4: Frequency acoustical energies variations for three points for the transverse excitation case; grey lines are the kinematic calculations; –o– lines are the 1/3 octave band averaged kinematic calculations; thick lines are the power flow results

Acknowledgment

The authors gratefully acknowledge P. Nicot and E. Garrigues from Dassault-Aviation, France, for their scientific, technical and financial support.

References

[1] O.M. Bouthier and R.J. Bernhard, Journal of Sound and Vibration, 'Simple models of the energetics of transversely vibrating plates', **182** 1, (1992).

[2] H. Kuttruff, Acustica, 'Energetic sound propagation in rooms', **83**, (1997).

[3] A. Le Bot, Journal of Sound and Vibration, 'A vibroacoustic model for high frequency analysis', **211** 4, (1998).

[4] Y.P. Guo, Journal of the Acoustical Society of America, 'Radiation from cylindrical shells driven by on-surface forces', **95** 4, (1994).

[5] Y.P. Guo, Wave Motion, 'Asymptotic solutions for helical wavenumbers of waves in fluid-loaded cylindrical shells', **22** , (1995).

[6] S.P. Timoshenko and S. Woinowsky-Krieger, Theory of plates and shells (Mac Graw Hill, 1970).

[7] M.N. Ichchou, A. Le Bot and L. Jezequel, Journal of Sound and Vibration, 'Energy models of one-dimensional, multi-propagative systems', **201** 5, (1997).

[8] A. Le Bot, M.N. Ichchou and L. Jezequel, Journal of Acoustical Society of America, 'Energy flow analysis for curved beams', **102** 2, (1997).

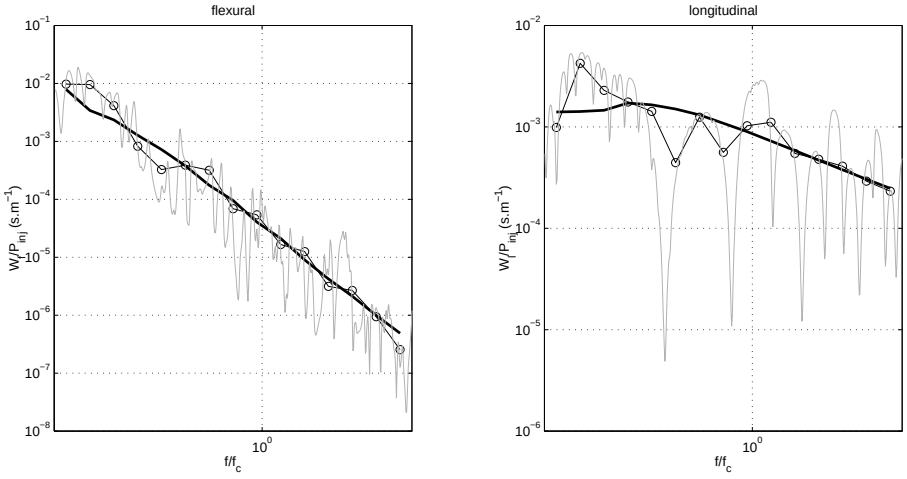

Figure 5: Frequency flexural and longitudinal energies variations for the tangential excitation case; grey lines are the kinematic calculations; –o– lines are 1/3 the octave band averaged kinematic calculations; thick lines are the power flow results

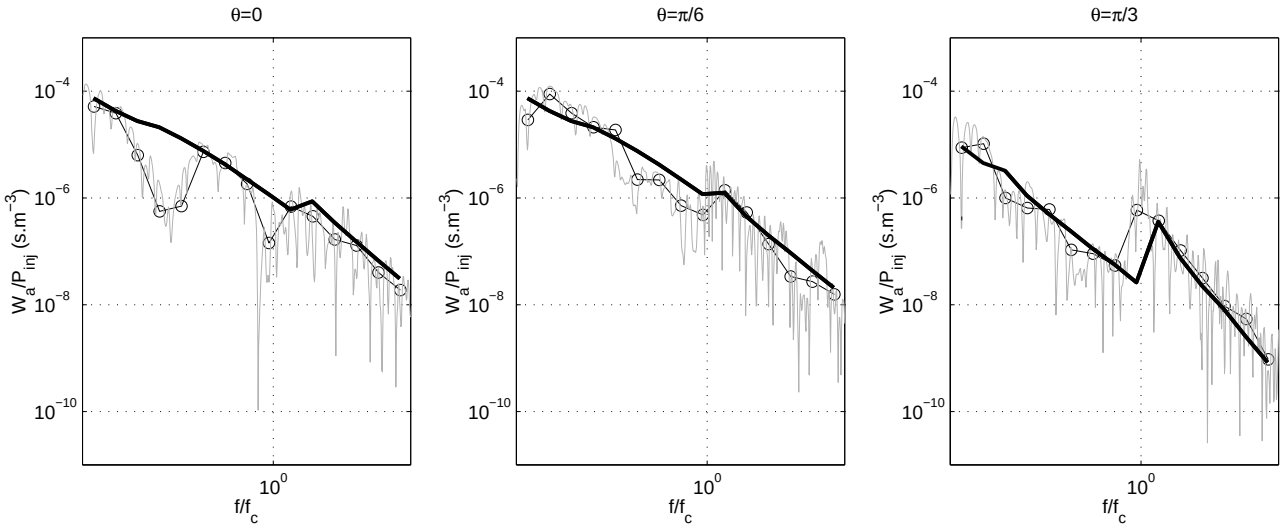

Figure 6: Frequency acoustical energies variations for three points for the tangential excitation case; grey lines are the kinematic calculations; –o– lines are the 1/3 octave band averaged kinematic calculations; thick lines are the power flow results